ELSEVIER

Journal of Hazardous Materials B137 (2006) 1600–1607

Journal of Hazardous Materials

www.elsevier.com/locate/jhazmat

Photooxidative *N*-de-ethylation of anionic triarylmethane dye (sulfan blue) in titanium dioxide dispersions under UV irradiation

Chiing-Chang Chen [a], Chung-Shin Lu [a], Fu-Der Mai [b,*], Chyan-Syang Weng [b]

[a] *Department of General Education, National Taichung Nursing College, Taichung 403, Taiwan, ROC*
[b] *Department of Applied Chemistry, Chung-Shan Medical University, Taichung 402, Taiwan, ROC*

Received 13 March 2006; received in revised form 26 April 2006; accepted 27 April 2006
Available online 30 May 2006

Abstract

The TiO_2-mediated photocatalysis process has been successfully applied to degradation of dye pollutants. Our results indicate that the TiO_2 surface is negatively charged, and the sulfan blue (SB) adsorbs onto the TiO_2 surface through the positive di-ethylamino groups while the TiO_2 surface is positively charged and the SB adsorbs onto the TiO_2 surface through the negative sulfonyl groups. In order to obtain a better understanding of the mechanistic details of this TiO_2-assisted photodegradation of the SB dye with UV irradiation, five intermediates of the processes were separated, identified, and characterized by the HPLC-ESI-MS technique, which included a positive- and negative-ion mode. The results indicated that the *N*-de-ethylation process continues until the *N*-de-ethylated SB dye is completely formed. The probable photodegradation pathways were proposed and discussed. The reaction mechanisms of UV/TiO_2 proposed in this study should be useful for future applications of the technology to the decolorization of dyes.

Keywords: UV/TiO_2; Triarylmethane; Sulfan blue; Dye; *N*-de-ethylation

1. Introduction

Synthetic textile dyes and other industrial dyestuffs constitute the largest group of chemicals produced in the word. In the dyeing process, 10–20% of dyes are reportedly lost to wastewater as a result of inefficiency [1]. Dyestuffs from the textile and photographic industries are becoming a major source of environmental pollution. The large amount of dyestuffs used in the dyeing stage of textile manufacturing represents an increasing environmental danger due to their refractory carcinogenic nature [2]. To de-pollute the dyeing wastewater, a number of methods have been investigated, including chemical oxidation and reduction, chemical precipitation and flocculation, photolysis, adsorption, ion pair extraction, electrochemical treatment, and advanced oxidation.

Advanced oxidation is one of the most promising technologies for the removal of dye-contaminated wastewaters due to its high efficiency. This technology is mainly based on the oxidative reactivity of $HO^{\bullet}$ radicals generated by various methods such as O_3/UV, H_2O_2/UV, H_2O_2/vis, O_3/H_2O_2/UV photolysis, photoassisted Fe^{3+}/H_2O_2, and TiO_2-mediated photocatalysis processes [3].

The TiO_2-mediated photocatalysis process has been successfully used to degrade pollutants during the past few years [4–16]. TiO_2 is broadly used as a photocatalyst because of its nontoxicity, photochemical stability, and low cost [17–20]. The initial step in the TiO_2-mediated photocatalysis degradation is proposed to involve the generation of an (e^-/h^+) pair, leading to the formation of hydroxyl radicals ($^{\bullet}OH$), superoxide radical anions ($O2^{\bullet-}$), and hydroperoxyl radicals ($^{\bullet}OOH$). These radicals are the oxidizing species in the photocatalytic oxidation processes. The efficiency of the dye degradation depends on the concentration of the oxygen molecules, which either scavenge the conduction band electrons (e^-_{cb}) or prevent the recombination of (e^-/h^+). The adsorbed dye molecules, leading to the formation of dye radical anions and the degradation of the dye, can pick up the electron in the conduction band [20].

Triarylmethane dyes are used extensively in the textile industry for dyeing nylon, wool, cotton, and silk, as well as for coloring of oil, fats, waxes, varnish, and plastics. The paper,

* Corresponding author. Tel.: +886 4 2473 0022; fax: +886 4 2324 8189.
E-mail address: davismai@csmu.edu.tw (F.-D. Mai).

0304-3894/$ – see front matter © 2006 Elsevier B.V. All rights reserved.
doi:10.1016/j.jhazmat.2006.04.047

leather, cosmetic, and food industries consume a high quantity of triarylmethane dyes of various kinds [1,21]. Additionally, the triarylmethane dyes are applied as staining agents in bacteriological and histopathological applications. The photocytotoxicity of triarylmethane dyes, based on the production of the reactive oxygen species, is tested intensively with the regard to their photodynamic treatment [22–24]. However, there is a great concern about the thyroid peroxidase-catalyzed oxidation of the triarylmethane class of dyes because the reactions might form various *N*-de-alkylated primary and secondary aromatic amines, the structures of which are similar to aromatic amine carcinogens [25].

In earlier reports [26–28], only one photodegradation of the anionic triarylmethane dyes, sulforhodamine-B, was investigated. The *N*-de-ethylation process was presumed to exist on the basis of the wavelength shift that occurs during the maximal absorption of the dyes. Only some of the photodegradation intermediates of this dye have been separated and identified, and the detailed mechanisms are still unclear. However, the photodegradation of SB dye has not been studied, and the intermediates have not been isolated or identified by the HPLC-ESI-MS technique.

Accordingly, identification of the reaction intermediates was performed using HPLC-ESI-MS, which reveals the degradation mechanism and reaction pathways of the photodegradation of SB dye in the UV/TiO_2 process, which in turn can serve as a foundation for future applications.

2. Experimental

2.1. Materials

The TiO_2 nanoparticles (P25, ca. 80% anatase, 20% rutile; particle size, ca. 20–30 nm; BET area, ca. 55 $m^2\,g^{-1}$) were supplied by Degussa. The SB dye was obtained from Tokyo Kasei Kogyo and used without further purification. The chemical structure of the SB dye is shown in Fig. 1. Stock solutions containing 1 g L^{-1} of SB dye in water were prepared, protected from light, and stored at 4 °C. HPLC analysis was employed to confirm the presence of the SB dye as a pure organic compound.

Reagent-grade ammonium acetate, sodium hydroxide, nitric acid, and HPLC-grade methanol were purchased from Merck.

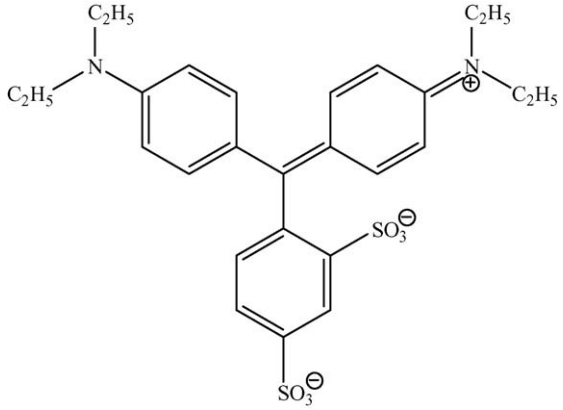

Fig. 1. Chemical structure of sulfan blue.

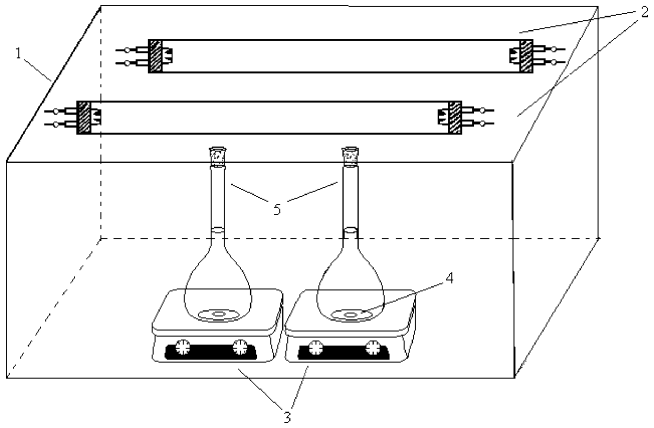

Fig. 2. Experimental apparatus: (1) C-75 Chromato-Vue cabinet of UVP, (2) UV-lamp, (3) magnetic stir, (4) stir bar, (5) 100 mL flask reactor.

De-ionized water was used throughout this study. The water was then purified with a Milli-Q water ion-exchange system (Millipore Co.) to give a resistivity of $1.8 \times 10^7\ \Omega$ cm.

2.2. Apparatus and instruments

The schematic of diagram of experimental apparatus was shown in Fig. 2. The C-75 Chromato-Vue cabinet of UVP provides a wide area of illumination from the 15-W UV-365 nm tubes positioned on two sides of the cabinet interior.

Waters ZQ LC/MS system, equipped with a binary pump, a photodiode array detector, an autosampler and a micromass detector, was used for separation and identification.

2.3. Procedures and analysis

An aqueous TiO_2 dispersion was prepared by adding 50 mg of TiO_2 powder to a 100 mL solution containing the SB dye at appropriate concentrations. For reactions in different pH media, the initial pH of the suspensions was adjusted by addition of either NaOH or HNO_3 solutions. Prior to irradiation, the dispersions were magnetically stirred in the dark for ca. 30 min to ensure the establishment of the adsorption/desorption equilibrium. Irradiations were carried out using two UV-365 nm lamps (15 W). At any given irradiation time interval, the dispersion was continues stirred, sampled (5 mL), centrifuged, and subsequently filtered through a Millipore filter (pore size, 0.22 μm) to separate the TiO_2 particles.

After each irradiation cycle, the amount of the residual dye was thus determined by HPLC-PDA. The analysis of organic intermediates was accomplished by HPLC-ESI-MS after the readjustment of the chromatographic conditions in order to make the mobile phase compatible with the working conditions of the mass spectrometer. Two different kinds of solvents were prepared in this study. Solvent A was 25 mM aqueous ammonium acetate buffer (pH 6.9) while solvent B was methanol instead of ammonium acetate. LC was carried out on an Atlantis™ dC18 column (250 mm × 4.6 mm i.d., dp = 5 μm). The flow rate of the mobile phase was set at 1.0 mL/min. A linear gradient was set as follows: $t = 0$, $A = 95$, $B = 5$; $t = 20$, $A = 50$, $B = 50$;

$t = 35$–40, $A = 10$, $B = 90$; $t = 45$, $A = 95$, $B = 5$. The column effluent was introduced into the ESI source of the mass spectrometer. Equipped with an ESI interface, the quadruple mass spectrometer with heated nebulizer probe at 350 °C was used with an ion source temperature of 120 °C. ESI was carried out with the vaporizer at 300 °C, nitrogen as sheath (80 psi), and auxiliary (20 psi) gas to assist with the preliminary nebulization and initiate the ionization process. A discharge current of 5 μA was applied. Tube lens and capillary voltages were optimized for the maximum response during perfusion of the SB standard.

Performed in flask without addition of TiO_2, the blank experiments show no appreciable decolorization of the irradiated solution, thus confirming the expected stability of this SB dye under UV light irradiation. Also, with addition of 0.5 g L^{-1} TiO_2 to solution, which contains 50 mg L^{-1} of the SB dye, the stability of the dye did not alter in the dark either.

3. Results and discussion

3.1. pH effect

In an aqueous system, TiO_2 is amphoteric [29]. The TiO_2 surface charge is predominantly negative when the pH is higher than the TiO_2 isoelectric point. As the pH decreases, the functional groups are protonated, and the proportion of the positively charged surface increases. Thus, the electrical property of the TiO_2 surface varies with the pH of the dispersion [30]. The surface of TiO_2 is negatively charged and adsorbs cationic species easily under pH > pHzpc (zero point charge) conditions while under the reverse conditions it adsorbs anionic ones. However, the adsorption of the substrate onto the TiO_2 surface directly affects the occurrence of electron transfer between the excited dye and TiO_2 and further influences the degradation rate. The surface becomes positively charged, and the number of adsorption sites may decrease above the isoelectric point of TiO_2. A similar effect by pH on the adsorption and photocatalytic reaction has been reported for Ag deposition [31] and the degradation of formic acid [32].

The photodegradation rate of the SB dye as a function of reaction pH is shown in Fig. 3. The rate was found to increase with decreasing pH values.

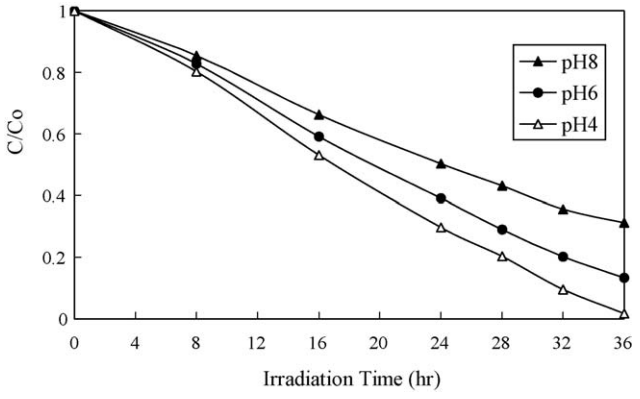

Fig. 3. pH effect on the SB photodegradation rate with concentrations of TiO_2 at 0.5 g L^{-1} and SB at 0.05 g L^{-1}.

With lower pH values, usually with the active •OH radicals formed at low concentration, electrostatic abstractive effects occurred between the positively charged TiO_2 particles and the operating anionic dyes by two sulfonyl groups, and hence the photodegradation process of SB remained much faster. Under basic conditions, the formation of active •OH species was favored, due partly to improved transfer of holes to the adsorbed hydroxyls, but also to the fact that the anionic SB dye was more difficult to adsorb onto the TiO_2 surface by the diethylamino group, which has a steric effect larger than the sulfonyl group, and hence the photodegradation process of SB was much slower.

These results indicate that when the TiO_2 surface is negatively charged, the SB adsorbs onto it through the positive diethylamino groups. When the TiO_2 surface is positively charged, the SB adsorbs onto it through the negative sulfonyl groups. A similar effect of the pH on the adsorption and photocatalytic reaction has been reported for the degradation of Sulforhodamine-B [27,33].

3.2. Effect of TiO_2 dosage

It is important from both the mechanistic and application points of view to study the dependence of the photocatalytic reaction rate on the concentration of TiO_2 in the SB dye. Hence, the effect of TiO_2 dosage on the photodegradation rate of the SB dye was investigated by employing different concentrations of TiO_2 varying from 0.25 to 2.0 g L^{-1}. As expected, the photodegradation rate of the SB was found to increase then decrease with the increase in the catalyst concentration (Fig. 4), a general characteristic of heterogeneous photocatalysts, and our results are in agreement with earlier reports [34]. It is known, however that the scattering light (around 1 g L^{-1}) has a practical limit, above which the degradation rate will decrease due to the reduction of the photonic flux within the irradiated solution.

3.3. UV–vis spectra

The aqueous solution of the SB dye was a little unstable under UV irradiation in the absence of TiO_2 (Fig. 4, 0 g curve).

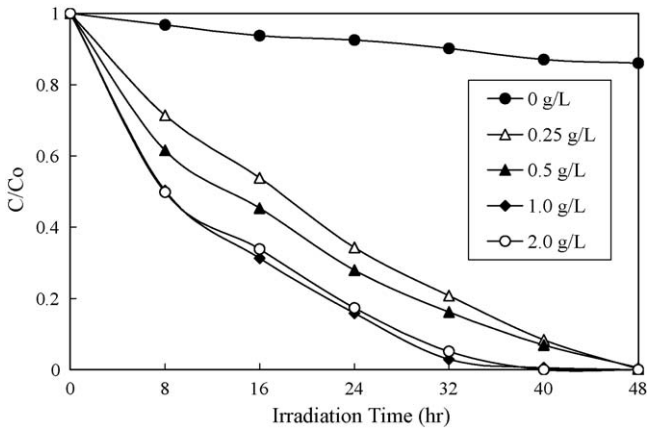

Fig. 4. Effect of TiO_2 dosage on the photodegradation rate for the decomposition of SB. Experimental conditions: dye concentration (0.05 g L^{-1}), irradiation time 48 h.

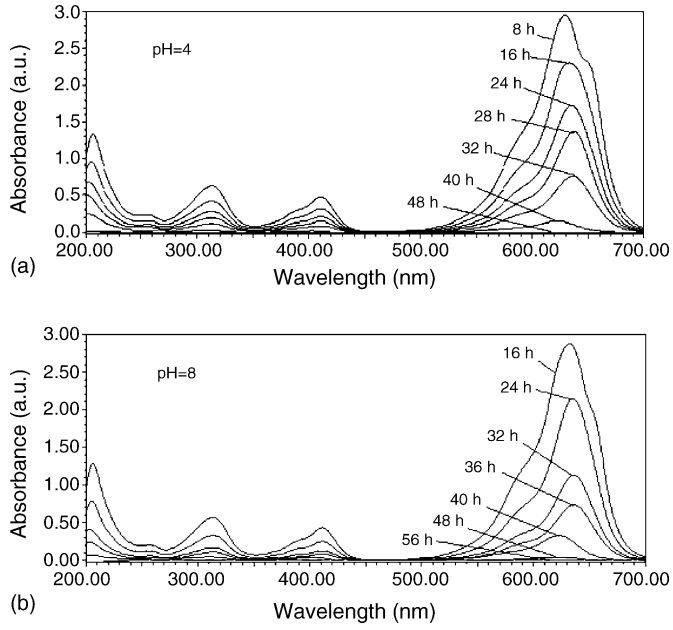

Fig. 5. UV–vis spectra changes of the SB dye in aqueous TiO_2 dispersions (SB 0.05 g L^{-1}, TiO_2 0.5 g L^{-1}) as a function of the irradiation time.

However, the SB dye can be degraded efficiently in aqueous SB/TiO_2 dispersions by UV irradiation at wavelength 365 nm. The changes of the UV–vis spectra during the photodegradation process of the SB dye in the aqueous TiO_2 dispersions under UV irradiation are illustrated in Fig. 5. About 99.9% and 99.8% of the SB dyes were degraded under the two following conditions: the former was at pH 4, after UV irradiation for 48 h; the latter was at pH 8, irradiation 56 h. In Fig. 5a and b, the characteristic absorption band of the dye around 632.5 and 630.1 nm decreased rapidly with slight hypsochromic shifts (621.8 and 622.1 nm), but no new absorption bands appeared even in the ultraviolet range ($200 < \lambda < 400$ nm). Thus, a series of *N*-de-ethylated intermediates may have formed, and either cleavage of the whole conjugated chromophore structure of the SB dye, or the degradation of the phenylic skeleton, or both may have occurred.

3.4. Separation and identification of the intermediates

Temporal variations occurring in the solution of the SB dye during the photodegradation process with UV irradiation were examined with HPLC, coupled with a photodiode array detector and ESI mass spectrometry. The chromatogram recorded at 580 nm is illustrated in Fig. 6. With irradiation up to 36 h, five components are identified, each with retention time under 50 min.

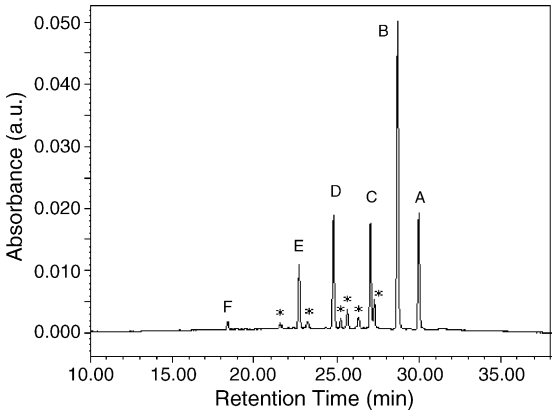

Fig. 6. HPLC chromatogram of the *N*-de-ethylated intermediates with 36 h of irradiation, at pH 8, recorded at 580 nm.

We denoted the SB dye and its related intermediates as species A–F (see Table 1 for detail). The *N*-de-ethylation of the SB has the wavelength position of its major absorption band moved toward the blue region, λ_{max}, A, 635.9 nm; B, 622.4 nm; C, 607.7 nm; D, 608.9 nm; E, 593.0 nm; F, 577.1 nm. The absorption spectra of each intermediate in the visible spectral region are depicted in Fig. 7; they are identified as A–F, corresponding to peaks A–F in Fig. 6, respectively. The absorption maximum

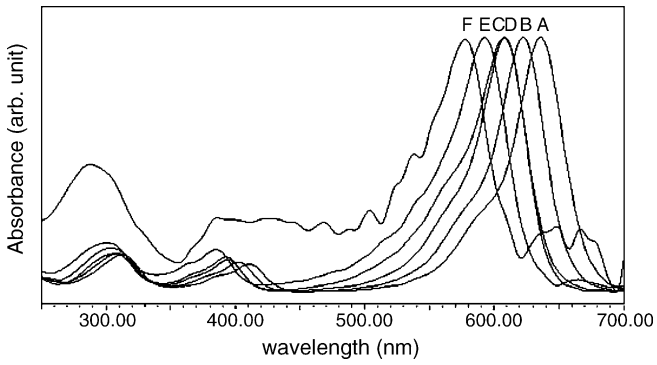

Fig. 7. Absorption spectra of the *N*-de-ethylated intermediates formed during the photodegradation process of the SB dye corresponding to the peaks in the HPLC chromatograph of Fig. 6. Spectra were recorded using the photodiode array detector. Spectra A–F correspond to the peaks A–F in Fig. 6, respectively.

Table 1
Identification of the *N*-de-ethylation intermediates of the SB dye by HPLC-ESI-MS

HPLC peaks	*N*-de-ethylation intermediates	Abbreviation	Retention time (min)	ESI-MS peaks (*m*/*z*)[a]	Absorption maximum (nm)
A	Sulfan blue	SB	30.198	545.11/543.10	635.9
B	*N*-de-mono-ethyl-sulfan blue	SB-M	28.918	517.10/515.09	622.4
C	*N*,*N*′-de-diethyl-sulfan blue	SB-MM	27.493	489.03/487.28	607.7
D	*N*,*N*-de-diethyl-sulfan blue	SB-D	25.955	489.09/487.21	608.9
E	*N*,*N*,*N*′-de-triethyl-sulfan blue	SB-DM	25.095	461.02/459.20	593.0
F	*N*,*N*,*N*′,*N*′-de-tetraethyl-sulfan blue	SB-DD	18.363	433.48/430.99	577.1

[a] Positive- and negative-ion ESI mass numbers (*m*/*z*).

of the spectral bands shifts hypsochromically from 638.5 nm (Fig. 7, spectrum A) to 578.3 nm (Fig. 7, spectrum F). This hypsochromic shift of the absorption band is presumed to result from the stepwise formation of a series of *N*-de-ethylated intermediates. The wavelength shifts are due to the *N*-de-ethylation of the SB dye caused by the attacks of some active oxygen species on the *N*,*N*-diethyl and *N*-ethyl groups. Similar phenomena were also observed during the photodegradation of rhodamine-B [35,36] and sulforhodamine-B [26–28] under visible irradiation. Additionally, the six weak peaks, designated with star marks, are depicted in Fig. 6. The absorption bands from 633.5 to 590.5 nm are observed. The absorption bands showed that the whole conjugated chromophore structure of the SB dye might exist. These intermediates were presumed to result from the formation of a series of *N*-hydroxyethylated intermediates [9] and/or phenylic ring hydroxylated dye derivatives [5].

The *N*-de-ethylated intermediates were further identified using the HPLC-ESI mass spectrometric method, and the relevant mass spectra are illustrated in Fig. 8. The molecular ion peaks appeared to be in the acid forms and basic forms of the intermediates. From the results of mass spectral analysis, we confirmed that the component A, $m/z = 545.11$ and $m/z = 543.10$, in liquid chromatogram was SB (Fig. 8, mass spectra A). The other components were B, $m/z = 517.10$ and $m/z = 515.09$, *N*-demono-ethyl-sulfan blue (Fig. 8, mass spectra B); C, $m/z = 489.03$ and $m/z = 487.28$, *N*,*N*′-de-diethyl-sulfan blue (Fig. 8, mass spectra C); D, $m/z = 489.09$ and $m/z = 487.21$, *N*,*N*-de-diethyl-sulfan blue (Fig. 8, mass spectra D); E, $m/z = 461.02$ and $m/z = 459.20$, *N*,*N*,*N*′-de-triethyl-sulfan blue (Fig. 8, mass spectra E); and F, $m/z = 433.48$ and $m/z = 430.99$, *N*,*N*,*N*′-de-tetraethyl-sulfan blue (Fig. 8, mass spectra F). Results of HPLC chromatograms, UV–vis spectra, and HPLC-ESI mass spectra are summarized in Table 1.

According to the number of the ethyl groups detached, we can characterize these intermediates. We found a pair of isomeric molecules, i.e., di-*N*-de-ethylated SB species, which differed only in their manner of loosening the ethyl groups from the benzyl groups. One of them, SB-MM, was formed by the removal of an ethyl group from two different benzyl groups of the SB molecule. Loosening two methyl groups from the same benzyl group of the SB dye produced the other one, SB-D. Therefore, considering the polarity of the SB-D species is greater than that of the SB-MM intermediates, we expected the latter to be eluted after the SB-D species. As well, to the extent that two *N*-ethyl groups are stronger auxochromic moieties than the *N*,*N*-diethyl or amino groups are, the maximal absorption of the SB-D intermediates was anticipated to occur at wavelengths shorter than the band position of the SB-MM species.

The relative distribution of the *N*-de-ethylated intermediates obtained is illustrated in Fig. 9. Except for the initial SB dye (peak A), the intensities of the other peaks increased at first and subsequently decreased, indicating the formation and transformation of the intermediates. To minimize errors, the relative intensities were recorded at the maximum absorption wavelength for each intermediate although a quantitative determination of the photogenerated intermediates was not achieved, owing to the lack of the appropriate molar extinction coefficients

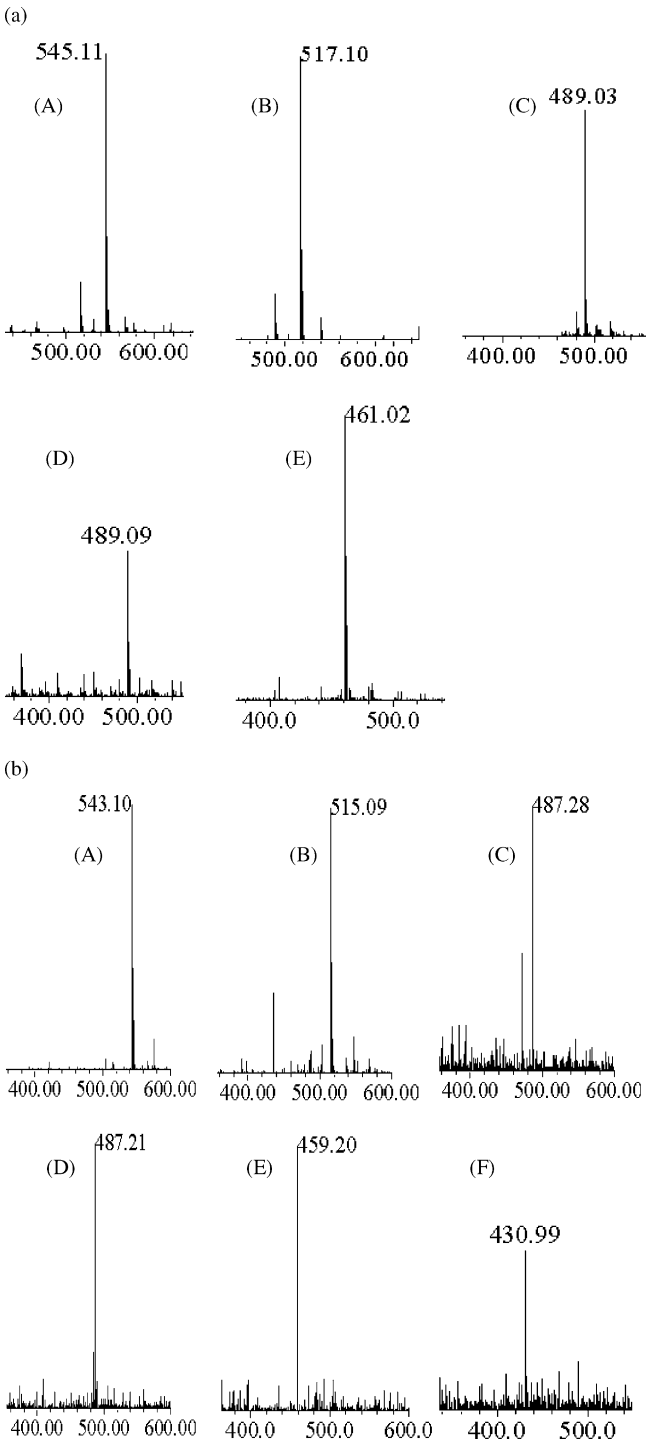

Fig. 8. ESI mass spectra of *N*-de-ethylated intermediates formed during the photodegradation of the SB dye after they were separated by HPLC-ESI-MS method: (a) Positive- and (b) negative-ion mass spectra, denoted A–F, correspond to the A–F species in Fig. 6, respectively.

of these intermediates and the related reference standards. The distributions of all of the *N*-de-ethylated intermediates are relative to the initial concentration of SB. Nonetheless, we clearly observed the changes in the distribution of each intermediate during the photodegradation process of the SB dye. In accordance with the data of Fig. 6, the successive appearance of the

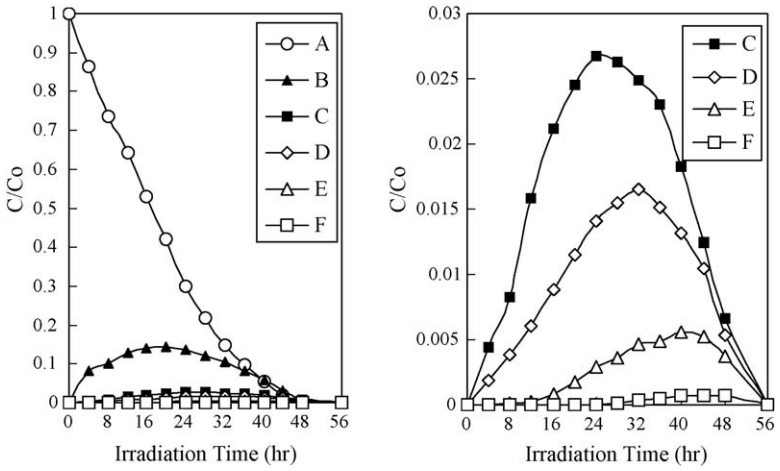

Fig. 9. Variation in the relative distribution of the *N*-de-ethylated products obtained from the photodegradation of the SB dye as a function of the irradiation time. Curves A–F correspond to the peaks A–F in Fig. 6, respectively.

maximal distribution of each intermediate indicates that the *N*-de-ethylation of SB is a stepwise photochemical process.

Under UV irradiation, most of the •OH radicals are generated directly from the reaction between the holes and surface-adsorbed H_2O or OH^-. $O_2^{-\bullet}$ should be much less likely to be formed than •OH [28]. The *N*-de-ethylation of the SB dye occurs mostly through the attack of the •OH species on the *N*,*N*-diethyl groups of the SB dye. Considering that the *N*,*N*-diethyl group in SB-M is bulkier than the *N*-ethyl group in SB-M molecules, the attack of •OH radicals on the *N*-ethyl groups should be favored at the expense of the *N*,*N*-diethyl groups. In accord with this notion, the HPLC results showed that the SB-D intermediates reached maximal concentration before the SB-MM intermediates did. The *N*-di-de-ethylated intermediates (SB-MM and SB-D) were clearly observed (Fig. 9, curve C–D) to reach their maximum concentrations after 24- and 20-h irradiation periods, respectively. The *N*-tri-de-ethylated intermediate (SB-DM) was clearly observed (Fig. 9, curve E) to reach its maximum concentration after a 40-h irradiation period. The *N*-tetra-de-ethylated intermediate (SB-DD) was clearly observed (Fig. 9, curve F) to reach its maximum concentration after a 44-h irradiation period. The successive appearance of the maximal quantity of each inter-

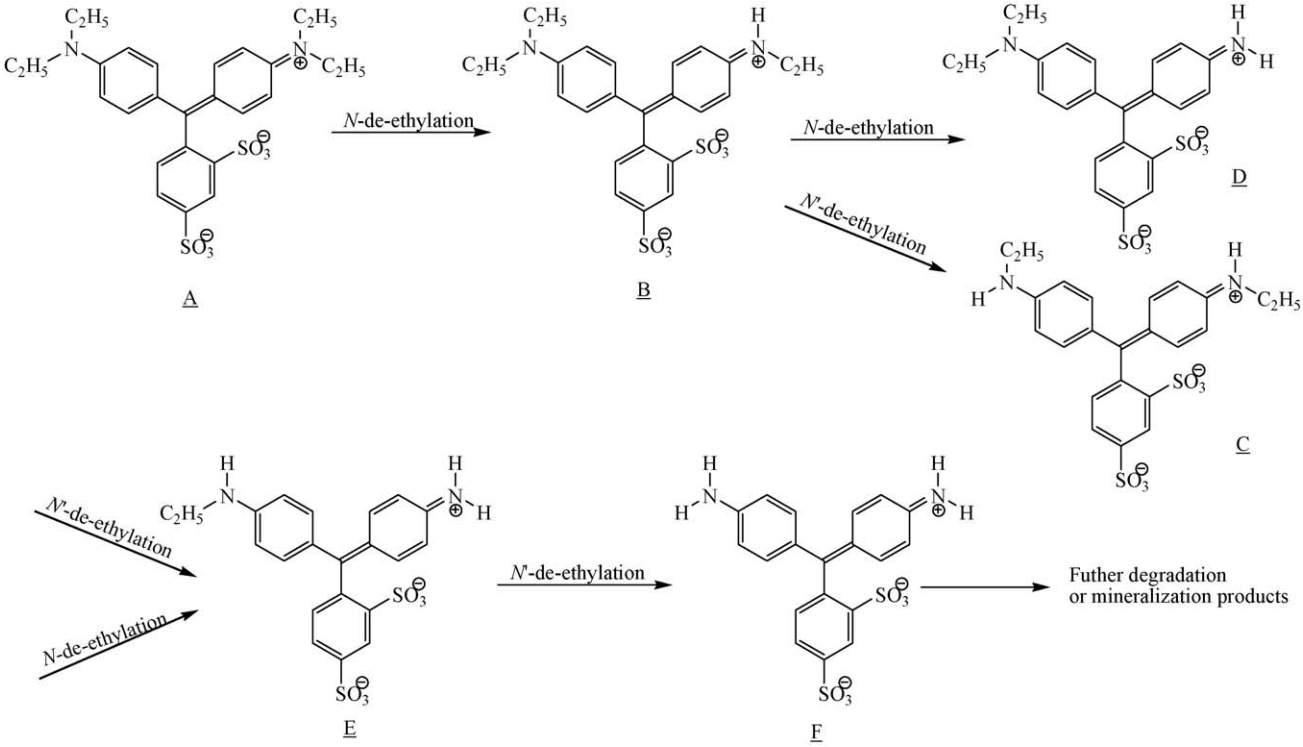

Scheme 1. Proposed *N*-de-ethylation mechanism of the SB dye under UV irradiation in aqueous TiO_2 dispersions followed by the identification of several intermediates by HPLC-ESI mass spectral techniques.

mediate indicates that the *N*-de-ethylation of SB is a stepwise photochemical process. The results we discussed above can be seen more clearly from Scheme 1.

According to earlier reports [37–39], most oxidative *N*-dealkylation processes are preceded by the formation of nitrogen-centered radical while destruction of the dye chromophore structures is preceded by the generation of the carbon-centered radical [33,36,40–42]. To be consistent with the above statement, the degradation of SB must occur via two different photooxidation pathways (destruction of the chromophore structure and *N*-de-ethylation) due to the formation of the different radicals (either carbon-centered radical or nitrogen-centered radical). There is no doubt that electron injection from the dye to the positive holes of TiO_2 yields the dye cationic radical. After this stage the cationic radical $Dye^{\bullet+}$ can undergo hydrolysis and/or deprotonation pathways of the dye cationic radicals, which in turn are determined by the different adsorption modes of SB on the TiO_2 particle surface.

On the basis of all the above experimental results, we tentatively propose the pathway of *N*-de-ethylation depicted in Scheme 1. The dye molecule in the SB/TiO_2 system is adsorbed through the positively charged diethylamine groups. Then the electrons are injected from the TiO_2 particle surface to the adsorbed dye through the positively charged diethylamine groups, and the subsequent hydrolysis (or deprotonation) yields a nitrogen-centered radical, which is then attacked by molecular oxygen to lead ultimately to *N*-de-ethylation. The mono-*N*-de-ethylated dye, SB-DM, can also be adsorbed on the TiO_2 particle surface and be involved in the other similar events (such as electron injection, oxygen attack and hydrolysis or deprotonation) to yield a bi-*N*-de-ethylated dye derivative, SB-D and SB-MM. The *N*-de-ethylation process as described above continues until formation of the completely *N*-de-ethylated dye, SB-DD. This indicates that the *N*-de-ethylation process predominates, and the cleavage of the conjugated structure occurs at a somewhat slower rate until all four-ethyl groups are removed.

When the SB dye molecules are located near the TiO_2 surface due to the sulfonyl group, which somewhat neutralizes the surface, the cleavage of the conjugated structure predominates during the initial stages. Destruction of the chromophore ring structure occurs mostly before full *N*-de-ethylation of the dye occurs.

4. Conclusion

The SB dye could be successfully decolorized and partially degraded by TiO_2 under UV irradiation. After 15 W UV-365 nm irradiation for 48 h, ca. 99.9% of SB was degraded. The photodegradation rate of the SB dye was found to increase along with decreases in the value of pH. However, the scattering light was shown to have a practical limit (around 1 g L^{-1}). Both *N*-de-ethylation and degradation of the SB dye take place in the presence of TiO_2 particles. The *N*-de-ethylation of the SB dye takes place in a stepwise manner with the various *N*-de-ethylated intermediate SB species. The *N*-de-ethylation process continues until formation of the completely *N*-de-ethylated dye. Besides, the ethyl groups are removed one by one as confirmed by the gradual wavelength shifts of the maximum-peaks toward the blue region. The hypsochromic effects resulting from *N*-de-ethylated intermediates of the SB dye occurred concomitantly during irradiation. The reaction mechanisms of TiO_2/UV proposed in this study should shed some light on future applications of the technology to the decoloration of dyes.

References

[1] Ullmann's Encyclopedia of Industrial Chemistry. Part A27. Triarylmethane and Diarylmethane Dyes, 6th ed., Wiley–VCH, New York, 2001.
[2] A. Reife, Dyes environmental chemistry, in: Kirk (Ed.), Othmer Encyclopedia of Chemical Technology, vol. 8, John Wiley and Sons Inc., New York, 1993.
[3] M.A. Fox, M.T. Dulay, Heterogeneous photocatalysis, Chem. Rev. 93 (1993) 341–357.
[4] C.C. Chen, C.S. Lu, Y.C. Chung, Photocatalytic degradation of ethyl violet in aqueous solution mediated by TiO_2 suspensions, J. Photochem. Photobiol. A: Chem. 181 (2006) 120–125.
[5] I.K. Konstantinou, T.A. Albanis, TiO_2-assisted photocatalytic degradation of azo dyes in aqueous solution: kinetic and mechanistic investigations: a review, Appl. Catal. B: Environ. 49 (2004) 1–14.
[6] H. Kyung, J. Lee, W. Choi, Simultaneous and synergistic conversion of dyes and heavy metal ions in aqueous TiO_2 suspensions under visible-light illumination, Environ. Sci. Technol. 39 (2005) 2376–2382.
[7] H. Mšt'ánková, J. Krýsa, J. Jirkovský, G. Mailhot, M. Bolte, The influence of Fe(III) speciation on supported TiO_2 efficiency: example of monuron photocatalytic degradation, Appl. Catal. B: Environ. 58 (2005) 185–191.
[8] C.C. Chen, X. Li, J. Zhau, H. Hidaka, N. Serpone, Effect of transition metal ions on the TiO_2-assisted photodegradation of dyes under visible irradiation: a probe for the interfacial electron transfer process and reaction mechanism, J. Phys. Chem. B 106 (2002) 318–326.
[9] N. Watanabe, S. Horikoshi, A. Kawasaki, H. Hidaka, N. Serpone, Formation of refractory ring-expanded triazine intermediates during the photocatalyzed mineralization of the endocrine disruptor amitrole and related triazole derivatives at UV-irradiated TiO_2/H_2O interfaces, Environ. Sci. Technol. 39 (2005) 2320–2326.
[10] N.M. Dimitrijevic, Z.V. Saponjic, B.M. Rabatic, T. Rajh, Assembly and charge transfer in hybrid TiO_2 architectures using biotin–avidin as a connector, J. Am. Chem. Soc. 127 (2005) 1344–1345.
[11] C.C. Chen, H.J. Fan, J.L. Jan, H.D. Lin, C.S. Lu, Photooxidative N-de-methylation of crystal violet dye in aqueous nano-TiO_2 dispersions under visible light irradiation, J. Photochem. Photobiol. A: Chem., doi:10.1016/j.jphotochem.2006.04.008.
[12] S. Rafqah, P.W. Chung, S. Nelieu, J. Einhorn, M. Sarakha, Phototransformation of triclosan in the presence of TiO_2 in aqueous suspension: mechanistic approach, Appl. Catal. B: Environ. 66 (2006) 119–125.
[13] T.V. Nguyen, H.C. Lee, O.B. Yang, The effect of pre-thermal treatment of TiO_2 nano-particles on the performances of dye-sensitized solar cells, Sol. Energy Mater. Sol. Cells 90 (2006) 967–981.
[14] N. Dubey, S.S. Rayalu, N.K. Labhsetwar, R.R. Naidu, R.V. Chatti, S. Devotta, Photocatalytic properties of zeolite-based materials for the photoreduction of methyl orange, Appl. Catal. A: Gen. 303 (2006) 152–157.
[15] Y.M. Wang, S.W. Liu, Z. Xiu, X.B. Jiao, X.P. Cui, J. Pan, Preparation and photocatalytic properties of silica gel-supported TiO_2, Mater. Lett. 60 (2006) 974–978.
[16] V. Iliev, D. Tomova, L. Bilyarska, A. Eliyas, L. Petrov, Photocatalytic properties of TiO_2 modified with platinum and silver nanoparticles in the degradation of oxalic acid in aqueous solution, Appl. Catal. B: Environ. 63 (2006) 266–271.
[17] A.J. Julson, D.F. Ollis, Kinetics of dye decolorization in an air-solid system, Appl. Catal. B: Environ. 65 (2006) 315–325.
[18] M. Muruganandham, N. Shobana, M. Swaminathan, Optimization of solar photocatalytic degradation conditions of reactive Yellow 14 azo dye in aqueous TiO_2, J. Mol. Catal. A: Chem. 246 (2006) 154–161.

[19] M.A. Fox, D.F. Duxbury, The photochemistry and photophysics of triphenylmethane dyes in solid and liquid media, Chem. Rev. 93 (1993) 381–433.
[20] M.R. Hoffman, S.T. Martin, W. Choi, W. Bahnemann, Environmental applications of semiconductor photocatalysis, Chem. Rev. 95 (1995) 69–96.
[21] H. Zollinger, Color Chemistry: Syntheses, Properties and Applications of Organic Dyes and Pigments, 2nd ed., VCH, Weinheim, 1991.
[22] M.S. Baptista, G.L. Indig, Effect of BS a binding on photophysical and photochemical properties of triarylmethane dyes, J. Phys. Chem. B 102 (1998) 4678–4688.
[23] L.M. Lewis, G.L. Indig, Effect of dye aggregation on triarylmethane-mediated photoinduced damage of hexokinase and DNA, J. Photochem. Photobiol. B: Biol. 67 (2002) 139–148.
[24] R. Bonnett, G. Martinez, Photobleaching of sensitisers used in photodynamic therapy, Tetrahedron 57 (2001) 9513–9547.
[25] B.P. Cho, T. Yang, L.R. Blankenship, J.D. Moody, M. Churchwell, F.A. Bebland, S.J. Culp, Synthesis and characterization of *N*-de-methylated metabolites of malachite green and Leucomalachite green, Chem. Res. Toxicol. 16 (2003) 285–294.
[26] W. Zhao, C.C. Chen, X. Li, J. Zhao, Photodegradation of sulforhodamine-B dye in platinized titania dispersions under visible light irradiation: influence of platinum as a functional co-catalyst, J. Phys. Chem. B 106 (2002) 5022–5028.
[27] C.C. Chen, W. Zhao, J.G. Li, J.C. Zhao, H. Hidaka, N. Serpone, Formation and identification of intermediates in the visible-light-assisted photodegradation of sulforhodamine-B dye in aqueous TiO_2 dispersion, Environ. Sci. Technol. 36 (2002) 3604–3611.
[28] G. Liu, X. Li, J. Zhao, H. Hidaka, N. Serpone, Photooxidation pathway of sulforhodamine-B. Dependence on the adsorption mode on TiO_2 exposed to visible light radiation, Environ. Sci. Technol. 34 (2000) 3982–3990.
[29] J. Zhao, H. Hidaka, A. Takamura, E. Pelizzetti, N. Serpone, Photodegradation of surfactants. 11. zeta-Potential measurements in the photocatalytic oxidation of surfactants in aqueous titania dispersions, Langmuir 9 (1993) 1646–1650.
[30] H.P. Boehm, Acidic and basic properties of hydroxylated metal oxide surfaces, Discuss. Faraday Soc. 52 (1971) 264–276.
[31] B. Ohtani, Y. Okugawa, S. Nishimoto, T. Kagiya, Photocatalytic activity of titania powders suspended in aqueous silver nitrate solution: correlation with pH-dependent surface structures, J. Phys. Chem. 91 (1987) 3550–3555.
[32] D.H. Kim, M.A. Anderson, Solution factors affecting the photocatalytic and photoelectrocatalytic degradation of formic acid using supported TiO_2 thin films, J. Photochem. Photobiol. A: Chem. 94 (1996) 221–229.
[33] X. Li, G. Liu, J. Zhao, Two competitive primary processes in the photodegradation of cationic triarylmethane dyes under visible irradiation in TiO_2 dispersions, New J. Chem. 23 (1999) 1193–1196.
[34] M. Saquib, M. Muneer, TiO_2-mediated photocatalytic degradation of a triphenylmethane dye (gentian violet), in aqueous suspensions, Dyes Pigm. 56 (2003) 37–49.
[35] T. Wu, G. Liu, J. Zhao, H. Hidaka, N. Serpone, Photoassisted degradation of dye pollutants. V. Self-photosensitized oxidative transformation of rhodamine B under visible light irradiation in aqueous TiO_2 dispersions, J. Phys. Chem. B 102 (1998) 5845–5851.
[36] J. Zhao, T. Wu, K. Wu, K. Oikawa, H. Hidaka, N. Serpone, Photoassisted degradation of dye pollutants. 3. Degradation of the cationic dye rhodamine B in aqueous anionic surfactant/TiO_2 dispersions under visible light irradiation: evidence for the need of substrate adsorption on TiO_2 particles, Environ. Sci. Technol. 32 (1998) 2394–2400.
[37] G. Galliani, B. Rindone, C. Scolastico, Selective de-methylation in the oxidation of arylalkylmethylamines with metal acetates, Tetrahedron Lett. (1975) 1285–1288.
[38] F.C. Shaefer, W.D. Zimmermann, Dye-sensitized photochemical autoxidation of aliphatic amines in non-aqueous media, J. Org. Chem. 35 (1970) 2165–2174.
[39] B.L. Laube, M.R. Asirvatham, C.K. Mann, Electrochemical oxidation of tropanes, J. Org. Chem. 42 (1977) 670–674.
[40] T. Wu, J. Lin, J. Zhao, H. Hidaka, N. Serpone, TiO_2-assisted photodegradation of dyes. 9. Photooxidation of a squarylium cyanine dye in aqueous dispersions under visible light irradiation, Environ. Sci. Technol. 33 (1999) 1379–1387.
[41] G. Liu, T. Wu, J. Zhao, K. Wu, K. Oikawa, H. Hidaka, N. Serpone, Photocatalytic degradation of dye sulforhodamine B: a comparative study of photocatalysis with photosenitization, New J. Chem. 24 (2000) 411–417.
[42] G. Liu, J. Zhao, K. Wu, K. Oikawa, H. Hidaka, N. Serpone, Photoassisted degradation of dye pollutants. 8. Irreversible degradation of alizarin red under visible light radiation in air-equilibrated aqueous TiO_2 dispersions, Environ. Sci. Technol. 33 (1999) 2081–2087.